

Isotropic and Aligned Stripe Phases in a Monomolecular Organic Film

M. Seul and V. S. Chen

AT&T Bell Laboratories, Murray Hill, New Jersey 07974

(Received 15 June 1992)

A novel transition has been investigated within the stripe phase of a monomolecular organic ("Langmuir") film. This transition mediates the transformation of an isotropic stripe liquid into an anisotropic state exhibiting twofold rotation symmetry. Stripe undulation and thickness fluctuations persist in the ordered state which also displays a high density of quenched topological defects. Stripe "melting" appears to coincide with the occurrence of thermal fluctuations which mediate the spontaneous breaking and rejoining of stripes, thereby altering the pattern connectivity.

PACS numbers: 68.10.-m, 61.30.Gd, 64.70.Md

The notion that competing interactions of differing range favor condensation into ground states in which the pertinent order parameter field exhibits periodic modulations has been widely invoked to account for domain formation. The simplest possible equilibrium configurations of such modulated phases, considered in mean-field theories incorporating a short-ranged attractive and a long-ranged repulsive interaction, are unidirectionally modulated ("stripe") and triagonally modulated ("bubble") phases [1,2]. The modulation period constitutes a new length scale which is set by the balance of pertinent competing free-energy contributions. In contrast to the ordered morphologies of the mean-field ground states, actual domain patterns, particularly those adopting a stripe morphology, observed under most conditions in thin slabs of such pertinent systems as ferrofluids [3], type I superconductors [4] and ferrimagnetic garnets [5], as well as in monomolecular amphiphilic ("Langmuir") films confined to an air-water interface [6], are disordered. Prominent among disordered stripe configurations are "labyrinthine" patterns [3-5] whose local structure has been recently analyzed in quantitative detail [7,8]. Of particular interest among disordered stripe patterns in the present context is an isotropic stripe phase, observed in two-component [9] as well as in single-component [10] Langmuir films, and previously referred to as a stripe liquid [9]. In contrast to the labyrinth patterns in magnetic and other systems, this isotropic stripe phase, to be described in more detail presently, exhibits the spontaneous breaking and rejoining of stripes, thus adopting local configurations in the form of fluctuating, branched clusters.

In this Letter we report the observation in a Langmuir film, i.e., in an essentially two-dimensional (2D) system, of a (reversible) transition between such a stripe liquid and an aligned stripe phase. The transition is characterized by the evolution of twofold rotation symmetry and by the emergence of a fixed pattern connectivity resulting from the suppression of fluctuations which mediate spontaneous stripe rupture. Small symmetry-breaking fields, notably flow, facilitate macroscopic alignment (over length scales of several hundred microns) along the preferred direction. The ordered state retains a high concen-

tration of topological defects including stripe "scissions," or "holes" ($-\cdot\cdot-$), as well as $-\frac{1}{2}$ ($-\cdot<$) and $+\frac{1}{2}$ ($\cdot-$) disclinations in the form of stripe "branch" and "end" points. This phase strongly resembles the 2D nematic [11] predicted within the context of defect-mediated melting of stripe phases in two dimensions [12, 13].

Domain patterns in monomolecular films composed of a binary mixture of the phospholipid dimyristoylphosphatidylcholine (DMPC) and cholesterol, and confined to an air-water interface, were rendered visible via fluorescence microscopy, relying on the preferential partitioning of 2 mole% of a fluorescent DMPC derivative between coexisting regions of different composition within the film [14]. The amphiphilic monolayer was maintained in a small Langmuir trough of rhombohedral geometry; its temperature was controlled in the range of 5°C and 22°C via thermoelectric devices encased in trough bottom and top cover. Images were recorded by means of a SIT video camera and stored on videotape or disk for subsequent processing and analysis [15].

The aligned stripe phase described here was observed in the phase diagram of Langmuir films containing binary mixtures of DMPC and cholesterol of near-critical composition in a range of temperatures between 5°C and 15°C: It is not accessible at room temperature. In addition, the range of molecular areas delineating the stripe regime, confined to a maximal interval between 46 Å² and 47 Å², is quite narrow. Locating the stripe phase in a film of fixed composition as temperature is varied requires knowledge of the temperature dependence of the critical composition. The requisite information is conveniently obtained by mapping the occurrences of the prevailing bubble type ("color") as a function of composition and temperature. This task entails preparation, at room temperature, of a film of the selected composition, its compression into, and equilibration for periods of hours in the homogeneous phase, its subsequent cooling to a desired temperature, and finally its expansion into the bubble regime. The crossover between the two different bubble morphologies delineates the regime of stripe morphology: It is mapped in the bottom panel of Fig. 1 and

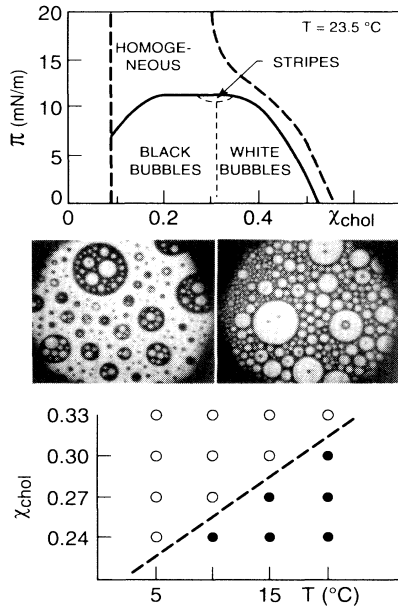


FIG. 1. Top: Phase diagram [14] of Langmuir films, composed of dimyristoylphosphatidylcholine (DMPC) and cholesterol, at a temperature of 23.5°C , exhibiting regimes of stripe and bubble domain formation. Middle: Examples of circular bubble domain patterns formed by the respective "minority" phase in the DMPC-rich (black bubbles) and in the cholesterol-rich (white bubbles) regime; the horizontal diameter of each field of view is approximately $200\ \mu\text{m}$. Bottom: Map of occurrence of prevailing bubble domain type (○ vs ●), indicating, in the form of the dashed line, the temperature dependence of the critical composition in DMPC-cholesterol binary mixed Langmuir films.

suggests a linear decrease of the critical composition with decreasing temperature.

A typical view of the stripe liquid phase observed in the immediate vicinity of the consolute point in the phase diagram of Fig. 1 is offered in Fig. 2, in conjunction with a sequence of three snapshots of the central portion of the pattern: These were taken in $\frac{1}{2}$ s intervals and enlarged twofold in the vertical panel of Fig. 2. This time sequence illustrates the fact that dynamic fluctuations enabling the rupturing and rejoining of stripes alter the pattern connectivity. That is, local configurations of the disordered stripe phase assume the topology of transient, branched stripe clusters, the spontaneous fluctuations in cluster connectivity facilitating the sampling of all (in-plane) directions. Consequently, the Fourier spectrum of this phase, exemplified by that shown as part of Fig. 4, is isotropic and typical of a liquid.

Provided that the Langmuir film has been equilibrated at an appropriate composition and temperature, as discussed above, slow, stepwise layer expansion (at typical rates of $\frac{1}{4}$ to $\frac{1}{2}$ $\text{\AA}^2/\text{molecule min}$) successively generates partially aligned and, in some areas of a given film, globally aligned stripes, such as those depicted in Fig. 3.

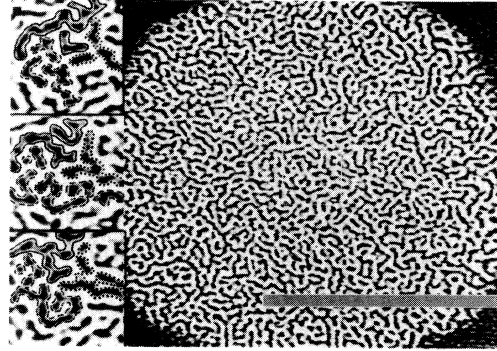


FIG. 2. Stripe liquid phase, recorded at $T \cong 10^\circ\text{C}$ and at a composition of 27 mole% cholesterol. The vertical panel contains three snapshots, twofold enlarged, of the central rectangular $25\ \mu\text{m} \times 33\ \mu\text{m}$ area marked in the main figure: Top and bottom enlargements, respectively, depict configurations of the central area $\frac{1}{2}$ s prior to and $\frac{1}{2}$ s subsequent to the middle image (and the main figure) and illustrate dynamic stripe rupturing ("pinch-off") fluctuations. The bar marks $100\ \mu\text{m}$.

The formation of such aligned patterns is apparently aided by the weak anisotropy of our rhombohedral Langmuir trough.

The evolution of twofold *orientational* ordering manifests itself in the form of azimuthal modulations in the intensity associated with the first peak in the Fourier spectrum computed from a given pattern. Pattern configurations corresponding to those of Figs. 2 and 3 yield the spectra displayed in Fig. 4. Each of the plots in Fig. 4 represents the (cyclic) autocorrelation function $i_Q(\phi) \equiv \langle I_Q(\phi) I_Q(0) \rangle$; $I_Q(\phi)$ is obtained by (numerically) performing an azimuthal scan of intensity over the radial interval $[Q - 1/2\Delta Q, Q + 1/2\Delta Q]$, centered at the position Q of the first peak in the Fourier spectrum.

Proceeding analogously as with the analysis of x-ray [16] and electron [17] diffraction data monitoring the onset of hexatic ordering in thin freely suspended liquid-crystal films, we model the autocorrelation function $i_Q(\phi)$ in terms of a Fourier series of the form

$$i(\phi) = i_0 \left\{ \frac{1}{4} + \sum_{n=1}^{\infty} c_{2n} \cos[2n(\pi - \phi)] \right\} + i_B,$$

the coefficients c_{2n} representing spectral densities and i_B denoting a dc background correction. The amplitude and coefficients of this series for $i_Q(\phi)$ are directly related to the corresponding quantities of the Fourier series representation of $I_Q(\phi)$, the function representing the original angular intensity modulations [18]. The fits so obtained yield the solid lines in Fig. 4, demonstrating that most of the data are well described by essentially a single mode and thus suggesting that the ordered state, exemplified by Fig. 3(b), remains in fact rather close to the transition. Further evolution of the orientational order, expected [16,17] to manifest itself in the appearance of higher har-

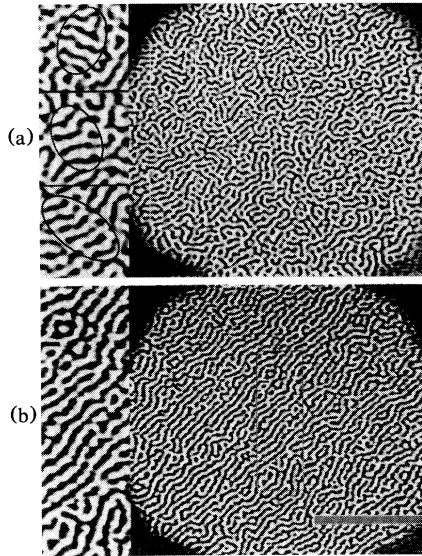


FIG. 3. (a) Partially aligned stripe phase, developing small regions in which stripe segments are aligned in a common direction; examples of such "cybotactic" clusters are shown in the vertical panels, depicting twofold enlargements of the rectangular areas marked in the main figure. (b) Globally aligned stripe phase containing "quenched" topological defects, such as "holes," i.e., pairs of free ends, "branches," and "ends" as well as "loops," visible in the vertical panel, containing a twofold enlargement of the $40\ \mu\text{m} \times 160\ \mu\text{m}$ central area marked in the main figure. Patches of aligned stripes have typical dimensions of hundreds of microns. Patterns were recorded at $T \cong 10^\circ\text{C}$ and at a composition of 27 mole% cholesterol. The bar marks $100\ \mu\text{m}$.

monics in response to the continued expansion of the film, is unfortunately preempted by a transition of the stripe into a bubble domain phase [9]: In fact, stripe alignment is observed only in immediate proximity to the stripe-bubble coexistence region.

The role of topological defects in the melting of a stripe phase in two dimensions has been analyzed within the framework of an elastic theory [12,13] which does not, however, take into consideration the spontaneous breaking of stripes and the resulting creation of free stripe ends. The finite energy E_D of free (unbound) *dislocations* in a two-dimensional stripe phase [1,12,13] implies the formation of a finite number, $n_D \sim \exp(-E_D/kT)$ of such defects at any finite temperature, $T > 0$, transforming the smectic into a nematic phase [13], and leading to the exponential decay of positional correlations [12]. This scenario leaves the nematic as the only ordered 2D stripe phase: Stripe configurations are envisioned [12,13] to contain anisotropic cybotactic clusters of longitudinal and transverse dimensions $\xi_{\parallel} \sim \xi_D^{4/3}$ and $\xi_{\perp} \sim \xi_D^{2/3}$, respectively, with $\xi_D = n_D^{-1/2}$. The pattern in Fig. 3(a) displays such clusters: Examples shown enlarged in the panel on the left of that figure suggest values for ξ_{\parallel} of the order of

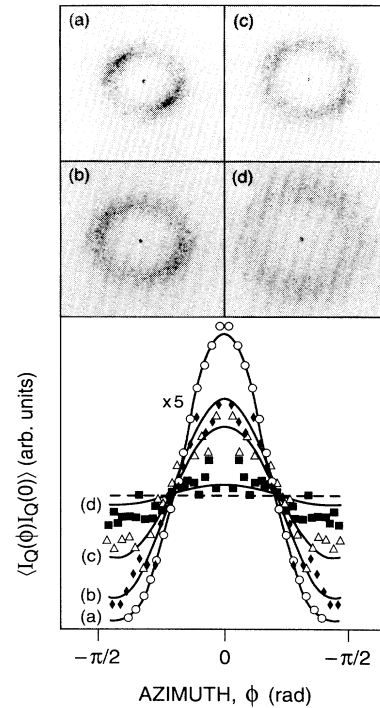


FIG. 4. Evolution of twofold orientational order marking the transition into aligned stripe phase: Shown are (cyclic) auto-correlation functions computed from $I_Q(\phi)$, with superimposed fits to the Fourier series discussed in the text. The fits yield the following values for the spectral densities: (c) $c_2=0.03$; (b) $c_2=0.06$; (a) $c_2=0.347$, $c_4=0.046$; the slight residual modulation in (d) results from an artifact in the evaluation of the 2D Fourier spectrum and, in $I_Q(\phi)$, is out of phase with the modulations manifest in (a)–(c). Also shown are Fourier spectra of disordered (\blacksquare) as well as partially (Δ , \blacklozenge) and globally (\circ) ordered stripe patterns such as those in Figs. 2 and 3: These spectra reveal the azimuthal intensity modulations analyzed in the main figure. Also visible is the significant shift in the position of the maximum, indicating a corresponding increase in the stripe period as the ordered state is approached.

5 modulation periods: A weak modulation in the corresponding function i_Q of Fig. 4 signals the onset of twofold orientational order.

This order is apparent in aligned patterns of the type displayed in Fig. 3(b), and manifests itself in the analysis summarized in Fig. 4. These latter patterns also display a significant increase in the decay length of orientational correlations. On length scales exceeding ξ_D , the 2D nematic phase [11–13] is predicted to exhibit algebraically decaying orientational correlations. Analysis is in progress to check this distance dependence. However, it is noteworthy that *positional* correlations probed by evaluating an azimuthally averaged 2D Patterson function (not shown here) exhibit typical correlation lengths of only a few modulation periods, indicating a more rapid

decay of positional as compared to orientational correlations even in the aligned state, a situation consistent with what is expected in the nematic (as well as in the hexatic) phase.

Remarkably, simple estimates give essentially identical values both for the density of free ends and for that of branches in partially ordered [Fig. 3(a)] and in aligned [Fig. 3(b)] stripe phases. This would suggest that the increased range of orientational correlations in the aligned phase may be primarily attributed to an increased stripe persistence length [19] presuming that an effective elastic theory, perhaps akin to current theories of semiflexible polymers [20], may in fact be devised to treat the stripe configurations of the present dipolar system. Encouraging in this context is the observation of features strikingly similar to the ones discussed here, in simulations of 2D microemulsions, based on a simple, local model Hamiltonian [21].

Figures 2 and 3 attest to the prevalence of topological defects in both disordered and ordered stripe phases. Simple estimates show that, irrespective of the state of ordering, stripe ends are encountered approximately 3 times more frequently than branches, implying a correspondingly lower energy of formation of the former type of "vertex." Stripe ends proliferate as the isotropic stripe liquid emerges: Estimated values for the density of free ends in the stripe liquid (Fig. 2) exceed, by an approximate factor of 2, those pertaining to the partially and globally aligned states (Fig. 3). Whether this defect proliferation actually mediates, or is in fact required to achieve (stripe) melting [22], or whether it constitutes a dynamic effect reflecting the rate of stripe breaking, a situation somewhat reminiscent of that pertinent to "living" polymers [23], is an interesting and currently unresolved question. In remarkable contrast to the globally isotropic "labyrinthine" patterns in magnetic films, evolving under constraints set by stripe connectivity and retaining well-defined local order [7,8], the stripe liquid described here constitutes a truly isotropic state in which topological constraints resulting from the pattern connectivity have been eliminated.

It is a pleasure to acknowledge enlightening conversations concerning the work presented here with R. Bruinsma, D. Huse, and R. Larson.

- [1] T. Garel and S. Doniach, *Phys. Rev. B* **26**, 325 (1982).
- [2] D. Andelman, F. Brochard, and J.-F. Joanny, *J. Chem. Phys.* **86**, 3673 (1987).
- [3] R. E. Rosensweig, M. Zahn, and R. J. Shumovich, *J. Magn. Magn. Mater.* **39**, 127 (1983); A. O. Tsebers and M. M. Maiorov, *Magnetohydrodynamics* **16**, 21 (1980).
- [4] T. E. Faber, *Proc. R. Soc. London A* **248**, 460 (1958).
- [5] J. A. Cape and G. W. Lehman, *J. Appl. Phys.* **42**, 5732 (1971); P. Molho, J. L. Porteseil, Y. Souche, J. Gouzerh, and J. C. S. Levy, *J. Appl. Phys.* **61**, 4188 (1987).
- [6] W. Heckl and H. Möhwald, *Ber. Bunsen-Ges., Phys. Chem.* **90**, 1159 (1986); H. Gaub, V. Moy, and H. M. McConnell, *J. Phys. Chem.* **90**, 1721 (1986); R. M. Weis and H. McConnell, *J. Phys. Chem.* **89**, 4453 (1985).
- [7] M. Seul, L. R. Monar, L. O'Gorman, and R. Wolfe, *Science* **254**, 1557 (1991); M. Seul, L. R. Monar, and L. O'Gorman, *Philos. Mag. B* **66**, 471 (1992).
- [8] M. Seul and R. Wolfe, *Phys. Rev. Lett.* **68**, 2460 (1992); *Phys. Rev. A* **46**, 7519 (1992); **46**, 7534 (1992).
- [9] M. Seul and M. J. Sammon, *Phys. Rev. Lett.* **64**, 1903 (1990); M. Seul, *Physica (Amsterdam)* **168A**, 198 (1990); *Adv. Mater.* **4**, 521 (1992).
- [10] S. Akamatsu and F. Rondelez, *C. R. Acad. Sci. Ser. 2* **313**, 599 (1991).
- [11] D. R. Nelson and R. A. Pelcovits, *Phys. Rev. B* **16**, 2191 (1977).
- [12] J. Toner and D. R. Nelson, *Phys. Rev. B* **23**, 316 (1981).
- [13] D. R. Nelson and J. Toner, *Phys. Rev. B* **24**, 363 (1981).
- [14] C. L. Hirshfeld and M. Seul, *J. Phys. (Paris)* **51**, 1537 (1990).
- [15] M. Seul, M. J. Sammon, and L. R. Monar, *Rev. Sci. Instrum.* **62**, 784 (1991).
- [16] J. D. Brock *et al.*, *Phys. Rev. Lett.* **57**, 98 (1986); *Z. Phys. B* **74**, 197 (1989); *Phys. Today*, **42**, No. 7, 52 (1989).
- [17] M. Cheng, J. T. Ho, S. W. Hui, and R. Pindak, *Phys. Rev. Lett.* **59**, 1112 (1987); **61**, 550 (1988).
- [18] Y. W. Lee, *Statistical Theory of Communication* (Wiley, New York, 1960).
- [19] P.-G. de Gennes, *Scaling Concepts in Polymer Physics* (Cornell Univ. Press, Ithaca, NY, 1979).
- [20] T. Odijk, *Macromolecules* **19**, 2313 (1986).
- [21] R. G. Larson (unpublished).
- [22] B. I. Halperin, in *Physics of Defects*, edited by R. Balian *et al.*, Proceedings of Les Houches Summer School Session XXXV (North-Holland, Amsterdam, 1981), Chap. 14.
- [23] M. E. Cates and S. J. Candau, *J. Phys. C* **2**, 6869 (1990).

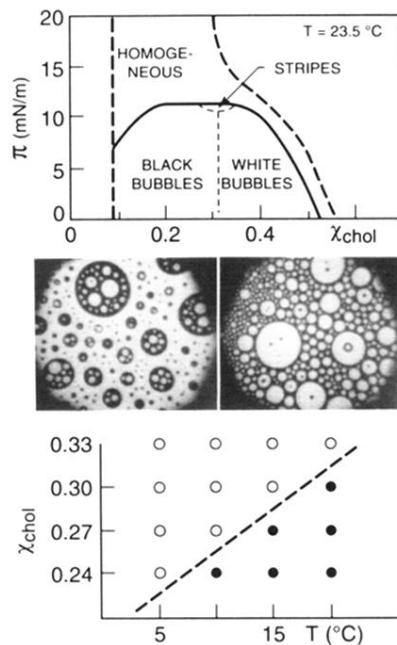


FIG. 1. Top: Phase diagram [14] of Langmuir films, composed of dimyristoylphosphatidylcholine (DMPC) and cholesterol, at a temperature of 23.5°C , exhibiting regimes of stripe and bubble domain formation. Middle: Examples of circular bubble domain patterns formed by the respective “minority” phase in the DMPC-rich (black bubbles) and in the cholesterol-rich (white bubbles) regime; the horizontal diameter of each field of view is approximately $200\ \mu\text{m}$. Bottom: Map of occurrence of prevailing bubble domain type (\circ vs \bullet), indicating, in the form of the dashed line, the temperature dependence of the critical composition in DMPC-cholesterol binary mixed Langmuir films.

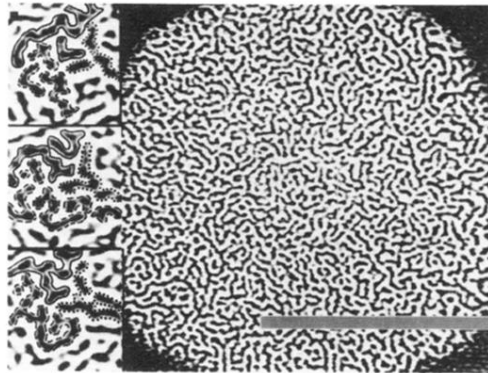


FIG. 2. Stripe liquid phase, recorded at $T \cong 10^\circ\text{C}$ and at a composition of 27 mole% cholesterol. The vertical panel contains three snapshots, twofold enlarged, of the central rectangular $25\ \mu\text{m} \times 33\ \mu\text{m}$ area marked in the main figure: Top and bottom enlargements, respectively, depict configurations of the central area $\frac{1}{2}$ s prior to and $\frac{1}{2}$ s subsequent to the middle image (and the main figure) and illustrate dynamic stripe rupturing (“pinch-off”) fluctuations. The bar marks $100\ \mu\text{m}$.

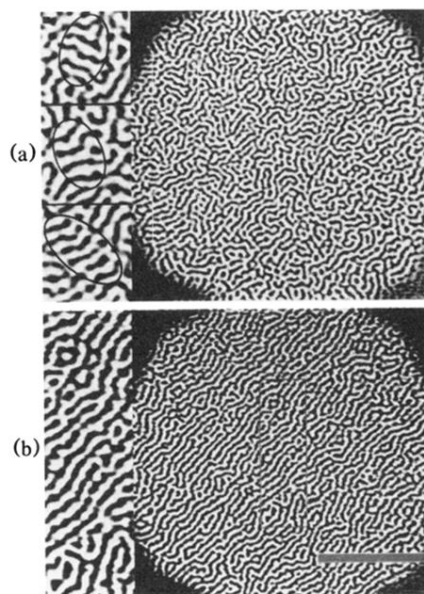


FIG. 3. (a) Partially aligned stripe phase, developing small regions in which stripe segments are aligned in a common direction; examples of such “cybotactic” clusters are shown in the vertical panels, depicting twofold enlargements of the rectangular areas marked in the main figure. (b) Globally aligned stripe phase containing “quenched” topological defects, such as “holes,” i.e., pairs of free ends, “branches,” and “ends” as well as “loops,” visible in the vertical panel, containing a twofold enlargement of the $40\ \mu\text{m} \times 160\ \mu\text{m}$ central area marked in the main figure. Patches of aligned stripes have typical dimensions of hundreds of microns. Patterns were recorded at $T \cong 10^\circ\text{C}$ and at a composition of 27 mole% cholesterol. The bar marks $100\ \mu\text{m}$.

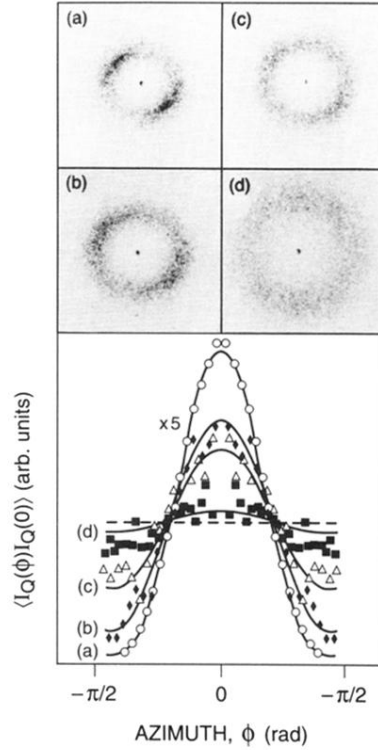


FIG. 4. Evolution of twofold orientational order marking the transition into aligned stripe phase: Shown are (cyclic) auto-correlation functions computed from $I_Q(\phi)$, with superimposed fits to the Fourier series discussed in the text. The fits yield the following values for the spectral densities: (c) $c_2=0.03$; (b) $c_2=0.06$; (a) $c_2=0.347$, $c_4=0.046$; the slight residual modulation in (d) results from an artifact in the evaluation of the 2D Fourier spectrum and, in $I_Q(\phi)$, is out of phase with the modulations manifest in (a)–(c). Also shown are Fourier spectra of disordered (■) as well as partially (Δ , \blacklozenge) and globally (\circ) ordered stripe patterns such as those in Figs. 2 and 3: These spectra reveal the azimuthal intensity modulations analyzed in the main figure. Also visible is the significant shift in the position of the maximum, indicating a corresponding increase in the stripe period as the ordered state is approached.